DMD Fast Forward. Published on October 12, 2012 as doi:10.1124/dmd.112.046342

DMD #46342

# Metabolism and quantification of [$^{18}$F]DPA-714, a new TSPO positron emission tomography radioligand

Marie-Anne Peyronneau, Wadad Saba, Sébastien Goutal, Annelaure Damont, Frédéric Dollé, Michael Kassiou, Michel Bottlaender and Héric Valette.

*Service Hospitalier Frédéric Joliot, CEA, I2BM, F-91406 Orsay, France: MAP, WS, SG, AD, FD, MB, HV.*

*Brain and Mind Research Institute, University of Sydney NSW 2050; School of Chemistry, University of Sydney NSW 2006, Discipline of Medical Radiation Sciences, University of Sydney NSW 2006: MK.*

DMD Fast Forward. Published on October 12, 2012 as DOI: 10.1124/dmd.112.046342
This article has not been copyedited and formatted. The final version may differ from this version.

DMD #46342

**Running title**: Metabolism of [$^{18}$F]DPA-714 in rodents and non human primates

**Correspondance:**

Marie-Anne Peyronneau

CEA, DSV, I2BM, Service Hospitalier Frédéric Joliot

4 Place du Général Leclerc, 91406 ORSAY, France.

E-mail : marie-anne.schollhorn@cea.fr

Phone : +33-1-69 86 77 52/Fax : +33-1-69 86 77 49

| | |
|---|---|
| Number of text pages: | 35 |
| Number of tables: | 2 |
| Number of figures: | 8 |
| Number of references: | 29 |
| Number of words in the abstract: | 254 |
| Number of words in the introduction: | 464 |
| Number of words in the Discussion: | 1468 |

**Abbreviations**:

[$^{18}$F]DPA-714: *N*,*N*-diethyl-2-(2-(4-(2-fluoroethoxy)phenyl) 5,7 dimethylpyrazolo[1,5a]pyrimidin-3-yl)acetamide

PET: Positron Emission Tomography

TSPO: 18kDa translocator protein

CYP: Human cytochrome P450

NADP: nicotinamide adenine dinucleotide phosphate

NADPH: nicotinamide adenine dinucleotide phosphate reduced form

G6P: glucose-6-phosphate

G6PDH: glucose-6-phosphate dehydrogenase

BCA: bicinchoninic acid

## Abstract

[$^{18}$F]DPA-714((*N*,*N*-diethyl-2-(2-(4-(2[$^{18}$F]-fluoroethoxy)phenyl)5,7dimethylpyrazolo[1,5a]pyri midin-3-yl)acetamide) is a new radioligand currently used for imaging the 18-kDa translocator protein in animal models of neuroinflammation and recently in humans. The biodistribution by PET in baboons and the *in vitro* and *in vivo* metabolism of [$^{18}$F]DPA-714 were investigated in rats, baboons and humans. Whole body PET experiments showed a high uptake of radioactivity in the kidneys, heart, liver and gallbladder. The liver was a major route of elimination of [$^{18}$F]DPA-714 and urine was a route of excretion for radiometabolites. In rat and baboon plasma, HPLC metabolic profiles showed three major radiometabolites accounting for 85% and 89% of total radioactivity at 120 min p.i., respectively. Rat microsomal incubations and analyses by LC/MS identified seven metabolites, characterized as O-deethyl, hydroxyl and N-deethyl derivatives of non-radioactive DPA-714, two of them having the same retention times than those detected in rat and baboon plasma. The third plasma radiometabolite was suggested to be a carboxylic acid compound that accounted for 15% of the rat brain radioactivity. *O*-deethylation led to a non radioactive compound and [$^{18}$F]fluoroacetic acid. Human CYP3A4 and CYP2D6 were shown to be involved in the oxidation of the radioligand. Finally an easy, rapid and accurate method -indispensable for PET quantitative clinical studies- for quantifying [$^{18}$F]DPA-714 by solid phase extraction was developed. *In vivo*, an extensive metabolism of [$^{18}$F]DPA-714 was observed in rats and baboons, identified as [$^{18}$F]deethyl, [$^{18}$F]hydroxyl and [$^{18}$F]carboxylic acid derivatives of [$^{18}$F]DPA-714. The main route of excretion of the unchanged radioligand in baboons was hepatobiliary while that of radiometabolites was the urinary system.

DMD Fast Forward. Published on October 12, 2012 as DOI: 10.1124/dmd.112.046342
This article has not been copyedited and formatted. The final version may differ from this version.



## Introduction

The 18-kDa translocator protein (TSPO) is a heteropolymeric mitochondrial protein (Scarf, 2011). TSPO is primarily located at outer mitochondrial membranes within transmembrane channels (Lacapere et al., 2003) that have many putative functions (Batarseh et al., 2010, Chelli et al., 2004, Rupprecht et al., 2010). TSPO is now known to have a widespread distribution in the organism (Hirvonen et al., 2010). Low levels of TSPO are found in the normal brain (Papadopoulos et al., 2006). TSPO is present in activated microglia (Myers et al., 1991), to a lesser extent in astrocytes and hence TSPO concentrations are found to be elevated in regions of brain inflammation arising from neurodegenerative disorders or stroke (James et al., 2008; Lang et al., 2002; Papadopoulos et al., 2006). Positron emission tomography (PET) imaging of the TSPO is therefore recognized as a clinical means to detect and investigate neuroinflammation. Among the PET radioligands which have reached a clinical use, [$^{11}$C]PK11195 has been the most widely used one (Hirvonen et al., 2010). New candidate PET ligands for TSPO have recently been developed (for review see Dollé et al., 2009) and these have been shown to have higher brain uptake and higher proportion of specific binding than [$^{11}$C]PK11195 (Lacapere et al., 2003, Chauveau et al., 2008). In a recent study of several animal models of brain inflammation in our institution, [$^{18}$F]DPA-714 ((*N*,*N*-diethyl-2-(2-(4-(2[$^{18}$F]-fluoroethoxy)phenyl)5,7dimethylpyrazolo[1,5a]pyrimidin-3-yl)acet amide) was shown to perform better than other tested radioligands such as [$^{11}$C]PK11195 and [$^{11}$C]DPA-713 (Chauveau et al., 2009). This finding suggested that [$^{18}$F]DPA-714 could be a promising agent for clinical TSPO imaging. [$^{18}$F]DPA-714 is now ongoing clinical development (Arlicot et al., 2012, Boellaard et al., 2011).

To date, identification of the radiometabolites of [$^{18}$F]DPA-714 has not been published. This is an important step in the development of a new radiotracer since the radiometabolite corrected arterial

input function for compartmental modelling is mandatory when no reference region (i.e. a region devoided of the target receptor) could be used. Furthermore, the presence of radiometabolites in the cerebral tissue could interfere with quantification. The quantification of TSPO distribution in the human brain requires the determination of the total plasma radioactivity concentration and the accurate determination of the non-metabolized fraction of [$^{18}$F]DPA-714 in plasma as a function of time. We have developed and validated a fast, sensitive and convenient approach using a solid phase extraction to quantify [$^{18}$F]DPA-714 in plasma. In addition, the equivalence of the time-activity curve at early time points of the PET study for the SPE procedure compared with our previous HPLC method is demonstrated.

The prediction of human metabolism, before starting clinical studies is also critical. Therefore, the metabolism of non radioactive DPA-714 was studied *in vitro* in microsomes (rat, baboon and human) and the metabolism of [$^{18}$F]DPA-714 was studied *ex vivo* in rats and *in vivo* in rats and baboons.

## Materials and methods

### Radiosynthesis

DPA-714 was labeled with fluorine-18 at its 2-fluoroethyl moiety using a tosyloxy-for-fluorine nucleophilic aliphatic substitution according to slight modifications of procedures already reported (Damont et al., 2008) and using a commercially available GE TRACERLab FX-FN synthesizer. Ready-to-inject, >99% radiochemically pure [$^{18}$F]DPA-714 (formulated in physiological saline containing less than 10% of ethanol), were obtained with specific radioactivities at the end of the radiosynthesis ranging from 37 to 111 GBq/µmol.

### In vivo metabolism of [$^{18}$F]DPA-714

### Animals

All animal use procedures were in strict accordance with the recommendations of the European Community (86/609/CEE) and the French National Committee (décret 87/848) for the care and use of laboratory animals. Four male adult Papio Anubis baboons (weight = 12.6 ± 4.3 kg) and male Sprague-Daley rats (weight = 250-300 g) were used.

### Stability of [$^{18}$F]DPA-714 in plasma and brain tissues

The radiochemical stability of [$^{18}$F]DPA-714 was checked *in vitro* in spiked rat or baboon plasma and rat brain homogenate at 37°C. A baboon blood sample was taken immediately before a PET study. Plasma was prepared by centrifugation (5 min, 3000 g, at room temperature). Six plasma samples (500 µL) were mixed with 20 kBq / mL of [$^{18}$F]DPA-714. Three of them were extracted with 700 µL of $CH_3CN$ (98% recovery). The extracts were injected onto the radio-HPLC system

DMD Fast Forward. Published on October 12, 2012 as DOI: 10.1124/dmd.112.046342
This article has not been copyedited and formatted. The final version may differ from this version.



and the peak area corresponding to [$^{18}$F]DPA-714 was measured (time zero). The other three plasma samples were incubated at 37°C for 190 min before extraction (same extraction yield) and analysis. Similar experiments were performed with rat plasma. The stability of [$^{18}$F]DPA-714 in rat brain was also checked according to the following procedure. Rat brain was excised (see below), placed in 1 mL of aqueous 0.1M potassium phosphate buffer (pH7.4) and was exposed for 20 s to an ultrasonic probe at 4°C. The brain homogenate was mixed with [$^{18}$F]DPA-714 (37 kBq). Three aliquots were extracted with $CH_3CN$ and analyzed as described above. The remainder of the homogenate was incubated at 37°C for 180 min and then mixed with 2 mL of $CH_3CN$ and centrifuged at 3000 g for 10 min. The supernatant was collected in three tubes and directly analyzed by radio-HPLC.

**Radiometabolites analysis**

***Baboons***

During the PET experiments performed in isoflurane anesthetized baboons for the characterization of kinetics of [$^{18}$F]DPA-714, 28 blood samples from each of the four baboons (1 mL; 6 independent PET experiments) were drawn from the femoral artery from 0 to 120 min after injection and immediately centrifuged at 4°C for 5 min at 3000 g to obtain cell-free plasma. The radioactivity in plasma samples (200 µL) was measured in a cross-calibrated gamma-counter (Cobra Quantum D5003; Perkin-Elmer) and expressed in Bq. All the values were corrected for fluorine-18 decay (109.7 min) till the injection time according to the following equation: +EXP(LN(2)*x/109.7)*y where x represents the time of counting and y the radioactivity measured at that time.

For the radiometabolite analysis, arterial plasma samples (7 samples of 500 µL) were counted, deproteinated with 700 µL of acetonitrile and centrifuged at 4°C for 2 min (3000 g). The

radioactivity in the resulting precipitate was counted for calculating the percent recovery of radioactivity in the acetonitrile. The whole supernatant was injected onto the radio-HPLC system. Baboon urine was collected at the end of the PET experiment (T0+180 min) using a Fowley catheter (NM Medical, France). Urine sample (1 mL) was directly injected onto the same radio-HPLC system.

The analytical system consisted of a quaternary gradient pump, an ASI100T autosampler and a UVD170U UV-Vis detector (Dionex, France) online with a LB-509 radioisotope detector (Berthold, La Garenne Colombes, France, MX Z500 cell). [$^{18}$F]DPA-714 and its radiometabolites were separated using a 5 µm, 10 x 250 mm, C18 SunFire$^{TM}$ preparative column (Waters, France). The mobile phases consisted of 0.1% trifluoroacetic acid in water (A) and 0.1% trifluoroacetic acid in acetonitrile (B). A linear gradient from 20% to 80% of B (and A from 80 to 20%) in 10 min was applied to the column at a flow rate of 5 mL/min (UV detection 220 nm). Data acquisition and processing were performed with Chromeleon software (version 1.0). The radioactivity due to unchanged [$^{18}$F]DPA-714 was expressed as a fraction of the total radiolabeled peak areas. The percentages of unchanged [$^{18}$F]DPA-714 in plasma as a function of time was fitted by a nonlinear regression analysis (Origin Pro software version 8.5) using a standard following bi-exponential decay equation.

***Rats***

Two rats were injected via a tail vein with 32.1 ± 2.8 MBq [$^{18}$F]DPA-714 and sacrificed by decapitation 120 min later. Plasma samples were treated and analyzed as described above. The whole brain was excised, weighed, counted and sonicated in 1 mL acetonitrile on ice. The homogenate was centrifuged 10 min at 3000 g. The pellet was resuspended and further sonicated in 1 mL acetonitrile. After centrifugation of the second homogenate, the two extracts were pooled and

DMD Fast Forward. Published on October 12, 2012 as DOI: 10.1124/dmd.112.046342
This article has not been copyedited and formatted. The final version may differ from this version.



concentrated by evaporation prior analysis by radio-HPLC. The concentrations of [$^{18}$F]DPA-714 and its radiometabolites in tissues were expressed as a percentage of injected dose per g of tissue (% ID/g). The radioactivity was also measured in the rat thighbone and in the bone marrow.

**Quantification of [$^{18}$F]DPA-714 in baboon plasma by solid phase extraction**

In order to develop a more sensitive, rapid and convenient method to isolate the unchanged radiotracer from its radiometabolites, a method using only solid phase extraction (SPE) was developed and compared to the radio-HPLC method, the latter being considered as the reference method. Five arterial plasma samples from each baboon (n=3) were counted and analysed by both radio-HPLC and SPE. A 60 mg HLB Oasis$^{TM}$ SPE cartridge (Waters, France) was conditioned with 1 mL of $CH_3OH$ and equilibrated with 5 mL of water. For the development of the method, the following procedure was used. Plasma samples (200 µL) were diluted to 400 µL with an aqueous solution of containing 4% chlorhydric acid. The radioactivity was measured in the resulting solution that was directly applied onto the HLB cartridge (SPE fraction F1). The cartridge was then sequentially washed with 1 mL of $H_2O$ (fraction F2), then with a $CH_3CN/H_2O$ solution (fraction F3). Several concentrations of $CH_3CN$ (fifteen concentrations between 25 and 39 %) were tested for elution of the last fraction of radiometabolites. Then, 1 mL of a $CH_3CN/H_2O$ 35/65 (v:v) solution was chosen for an optimal separation. [$^{18}$F]DPA-714 was finally eluted with 1 mL of $CH_3CN$ (fraction F4). The radioactivity was measured in all the collected fractions as well as in the cartridge (fraction F5). The last fraction (fraction F6) represents the empty tip and tube containing few amounts of plasma that was not applied on the cartridge. The radioactivity due to unchanged [$^{18}$F]DPA-714 was expressed in percent of the sum of radioactivity found in the eluted fractions or as a fraction of the initial radioactivity measured in each plasma sample.

DMD Fast Forward. Published on October 12, 2012 as DOI: 10.1124/dmd.112.046342
This article has not been copyedited and formatted. The final version may differ from this version.



### Major routes of [$^{18}$F]DPA-714 excretion in baboons

The main routes of excretion of [$^{18}$F]DPA-714 were studied using whole body PET imaging (HR+ PET tomograph, Siemens, Tn). Transmission scans (3 min per step, 5 or 6 steps according to the height of the animal) in 2D mode were used for subsequent correction of attenuation of emission scans. Emission scans (in 3D-mode, increasing duration from 1 to 4 min per step) were performed up to 90 min following *i.v.* injection of 276 ± 60 MBq (4.8 ± 2.1 nmol) of [$^{18}$F]DPA-714. VOIs were drawn over all organs presenting a significant radioactivity by an experienced investigator on the earliest emission image for liver, gallbladder, spleen, kidneys, and vertebral bodies. For the urinary bladder, a VOI was drawn on the last emission image.

## ***In vitro*** **metabolism of DPA-714**

### Chemicals

D-glucose-6-phosphate disodium salt (G-6-P), beta-nicotinamide adenine dinucleotide phosphate (NADPH), glucose-6-phosphate dehydrogenase (G6 PDH) from yeast, formic acid and bicinchoninic acid (BCA) protein assay kit were purchased from Sigma-Aldrich (St Quentin Fallavier, France). Solvents used for HPLC and LC-MS-MS analyses were from VWR (Val de Fontenay, France).

### Liver microsomes and cDNA-expressed human P450s

Microsomes from adult male Sprague-Dawley rats and from baboons were prepared by homogenization of liver samples over ice in a 0.1M aqueous Tris-HCl buffer (pH 7.4) containing 1 mM EDTA and 0.2 M sucrose, followed by differential centrifugations according to Kremer's method (Kremers et al., 1981). Total P450 content was spectrophotometrically measured (Omura

et al., 1964). Total microsomal proteins content was determined according to the method of BCA using serum albumin as standard. Rats were sacrificed one day after the last administration of the inducer. Human liver microsomes (pool of 10 individuals) and insect cell microsomes containing recombinant baculovirus cDNA-expressed human P450 (CYP1A2, CYP2A6, CYP2B6, CYP3A4, CYP2C8, CYP2C9, CYP2C19, CYP2D6 and CYP2E1 and CYP3A4 supersomes) characterized for their P450 content, protein content and main specific catalytic activities were purchased from Gentest Corp (BD Biosciences, France). All microsomal fractions were stored at -80°C until used.

**Typical microsomal incubation procedure**

Incubations contained 1 mg of microsomal proteins (rat, baboon and human liver microsomes), a NADPH-generating system (5 mM G6P, 1 mM $NADP^+$, G6P dehydrogenase 2UI), DPA-714 (100 µM) and 0.1 M aqueous potassium phosphate buffer (potassium dihydrogen phosphate and dipotassium hydrogen phosphate, pH 7.4) in a final volume of 1 mL. The reaction mixtures were preincubated for 2 min at 37°C prior to initiation of the reaction by the NADPH generating system. The incubations were conducted in a 37°C water bath with gentle shaking for 15, 30 and 60 min. The reaction was stopped by the addition of an equal volume of acetonitrile. Samples were centrifuged at 4°C for 5 min at 9000 g. The resulting supernatant was filtered (Vecta Spin Micro 0.2µm, Whatman, France) and 20 µL were analyzed by LC-MS-MS as described herein. Controls were incubated either without NADPH-generating system or without microsomes in order to ensure the stability of the tracer in the experimental conditions. The percentage of each metabolite was determined as a percentage of the total peak area. Enzymatic catalytic activities are expressed as a formation rate of each metabolite in nmol per milligram of microsomal proteins per min (nmol metabolite/ mg/ min).

**Oxidation of DPA-714 by cDNA-expressed human P450s isoforms**

DMD Fast Forward. Published on October 12, 2012 as DOI: 10.1124/dmd.112.046342
This article has not been copyedited and formatted. The final version may differ from this version.



Microsomes from baculovirus-infected insect cells expressing human CYPs and cell microsomes containing control activity were used (Gentest Corp., BD Biosciences, France) to test their ability to oxidize DPA-714. Incubations included DPA-714 (50 µM), 20 pmol of CYP, 1.3 mM $NADP^+$, 3.3 mM G-6-P, G6PDH 2UI and 0.1 M aqueous phosphate buffer (pH 7.4) in a final volume of 500 µL. The reaction proceeded for 30 min at 37°C and was stopped by the addition of 500 µL acetonitrile. Samples were centrifuged for 5 min at 10,000 g and 20 µL of the supernatants were analyzed by LC-MS-MS. Results are expressed as a percentage of the total peak areas for each metabolite (% of biotransformation).

**Identification of DPA-714 metabolites by LC- MS-MS**

DPA-714 metabolites were analyzed by LC-MS-MS in microsomal extracts on a LCQ Deca XP+ ion trap mass spectrophotometer equipped with an electrospray source (Thermo Electron, les Ulis, France). The HPLC system interfaced with the LCQ Deca XP+ consisted of a LC pump Surveyor (series 54949), PDA Surveyor (series 56470) and a Surveyor autosampler (series 55989, Thermo Electron, Les Ulis, France). Pressurized nitrogen was used as sheath gas with a flow rate of 25 units (arbitrary units for sheath gas pressure as defined by the manufacturer). The source voltage for electrospray ionization was 4.5 kV and the capillary voltage was 38 V. The capillary temperature was 275°C. The separation of DPA-714 and its metabolites was performed using a reverse phase Atlantis C18 column 2.1x150 mm, 5 µm (Waters, Saint-Quentin, France). The mobile phase consisted of A: $H_2O$ containing 0.05% formic acid and B: acetonitrile containing 0.05% formic acid. A linear gradient from 20 to 70% of B (80 to 30% of A) in 30 min was applied to the column at a flow rate of 200 µL/ min. The whole output of the LC column was introduced into the photodiode array detector (190-600 nm) before electrospray ionization probe of the LCQ Deca XP+ operated in the positive mode. In the full scan MS acquisition mode, the instrument method was set up to detect ions

in the range of *m/z* 50-500. The MS was set up in the MS-MS mode for acquiring, isolating with a mass width of 1 Da and dissociating the ion *m/z*=399 and its main metabolites by Collision Induced Dissociation in the ion trap using helium as the collision gas with an energy of 35%. Data acquisition and processing were performed with Xcalibur™ software (version 2.0) with the assistance of Mass Frontier™ software (version 4.0) for proposed fragmentation mechanisms (Thermo Electron, les Ulis, France).

## Results

### In vivo studies

#### Stability of [$^{18}$F]DPA-714 in plasma and brain tissues

[$^{18}$F]DPA-714 proved to be stable in saline and upon incubation of spiked baboon plasma at 37°C for 190 min. Indeed, no decomposition products could be observed for [$^{18}$F]DPA-714 by radio-HPLC analysis. [$^{18}$F]DPA-714 also proved to be stable in rat plasma and brain homogenate for 180 min at 37°C.

#### In vivo metabolism in baboons

Radio-HPLC profiles of plasma extracts showed three main radiometabolite peaks along with [$^{18}$F]DPA-714 with retention times at 3.2 min, 7.2 min, 8.6 min and 10 min respectively (Fig.1). The percentage of non-metabolized [$^{18}$F]DPA-714 rapidly and exponentially decreased as a function of time (Fig.2A) representing 46% at 30 min and only 11% at 120 min post-injection. During the same time, the percentage of the main radiometabolite [$^{18}$F]-M7 increased and reached 50% of plasma radioactivity (Fig.2A). The radioactivity measured in the acetonitrile protein precipitates (acetonitrile pellet) increased as a function of time and accounted for 17% of total plasma radioactivity at 120 min (Fig. 2B). This radioactivity may be due to the presence of [$^{18}$F]fluoroacetate (or [$^{18}$F]fluoroacetic acid) generated by *O*-dealkylation of the tracer. This fraction was considered as a radiometabolite for the quantification of [$^{18}$F]DPA-714 in plasma and the determination of the time-course of the radioligand (Fig.2A). The plasma concentrations of radioactivity and non-metabolized [$^{18}$F]DPA-714 are presented in Fig. 2C (input function and metabolite-corrected input function).

In urine, the same radiometabolites than those detected in plasma were observed along with a very

DMD Fast Forward. Published on October 12, 2012 as DOI: 10.1124/dmd.112.046342
This article has not been copyedited and formatted. The final version may differ from this version.



few amount (less than 2%) of [$^{18}$F]DPA-714 at 180 min. The radiometabolites eluted at 3.2 min, 5.9 and 8.2 min represented 51%, 30% and 17% of total radioactivity, respectively (data not shown).

**Major route of [$^{18}$F]DPA-714 excretion in baboons**

SUVmax values obtained by whole body PET studies in baboons are summarized in Table 1. High uptake of radioactivity was observed in TSPO-rich regions such as heart (SUVmax= 7.42), parotid gland (SUVmax= 1.93). The highest radioactivity was observed in the kidneys: SUVmax 12.7 at 10 min post-injection, followed by a wash-out (SUV= 4.6 at 90 min p.i.). Brain displayed low radioactivity in these normal baboons. Vertebral bodies showed also an uptake of radioactivity (SUVmax =1.99 at 90 min p.i.) with a slow increase from the beginning untill the end of the PET experiment. One route of excretion was the hepatobiliary system: SUVmax in the gallbladder was 7.3 at 42 min p.i. followed by the appearance of a large amount of radioactivity in the duodenal area. The other route of excretion was the urinary bladder with a SUVmax of 6.5 at 90 min p.i.

**Quantification of [$^{18}$F]DPA-714 and its radiometabolites by solid phase extraction**

In the aim of developing a rapid, sensitive and accurate quantification method of [$^{18}$F]DPA-714 and its radiometabolites in plasma for human quantitative imaging studies, we have developed an approach using only solid phase extraction. In baboon spiked plasma, the yield of extraction of non-metabolized radiotracer was 95 ± 2 % (n=10). Limit of detection (LOD) and limit of quantification (LOQ) values were calculated as 1.2 and 1.8 Bq, compared to 55 and 145 Bq with HPLC. The mean total recovery of plasma samples radioactivity with this method was 94 ± 4 % (n=87). The time-activity course of SPE fractions are presented in fig.3A. The first fraction

corresponded to proteins and radiometabolites that were not retained on the SPE column by hydrophobic and anionic interactions. Polar radiometabolites were eluted in water (fraction F2). More hydrophilic radiometabolites were eluted with 35% acetonitrile/water (fraction F3). Non-metabolized [$^{18}$F]DPA-714 was eluted in the acetonitrile fraction as verified by radio-HPLC analysis (fraction F4). Figure 3C compares the time-course of unchanged radiotracer measured by SPE and radio-HPLC in plasma samples of three different baboons. The percentage of unchanged [$^{18}$F]DPA-714 followed a similar exponential decrease with both techniques (Fig.3B).

**In vivo metabolism in rats**

Rat plasma samples analyses demonstrated the formation of three radiometabolites having the same retention times than those detected in baboons. In plasma at 120 min post injection, the concentration of non-metabolized [$^{18}$F]DPA-714 was 15% of the total radioactivity (Fig.4). The main radiometabolite was suggested to be generated in plasma by further oxidation of hydroxylated radiometabolite(s) into a carboxylic acid derivative ([$^{18}$F]-M7, see identification of metabolites). This radiometabolite accounted for most of the plasma radioactivity. In the brain, at the same time, the concentration of total radioactivity was 2-fold higher than in plasma while that of non-metabolized [$^{18}$F]DPA-714 was 11-fold higher than in plasma. This fraction represented 85% of the total brain radioactivity (Fig.4). The radiometabolite [$^{18}$F]-M7 represented 15% of the total brain radioactivity. However, the concentration of [$^{18}$F]-M7 was lower than in plasma (ratio of 0.4). The concentrations of the other radiometabolites found in plasma were quantitatively negligible in brain tissue. The radioactivity was also measured in the cortex of the thighbone and in the bone marrow at 120 min post-injection. The results showed that 65% of the total bone radioactivity was in the bone marrow and 35% was found in the cortex of the thighbone.

## In vitro studies

### Species comparison

Representative HPLC chromatograms of rat and human microsomal incubates are shown in fig.5A. Seven metabolites more polar than DPA-714 generated from oxidation by cytochromes P450 were detected in rat liver microsomal incubations by LC-MS (M1 to M6b; Fig.5A). The formation rates for each metabolite expressed in nmol/mg/min were compared in three species (Fig.5B). Rat liver microsomes catalyzed the formation of five metabolites M1 to M6b, M1 and M3 being the most abundant (0.89 and 0.82 nmol/mg/min) followed by M2, M4, M5. In baboon liver microsomes, M4 and M5 were the predominant metabolites (0.46 and 0.64 nmol/mg/min) while they were M3 and M4 in human liver microsomes (0.45 and 0.57 nmol/mg/min). It should be noticed that all the metabolites except M5 would remain radioactive with [$^{18}$F]DPA-714.

### Identification of DPA-714 metabolites

Positive ions ESI-MS and the major MS-MS fragments obtained for each metabolite (M1 to M6b) detected in microsomal fractions are summarized in Table 2. The mass spectrum of DPA-714 exhibited a molecular ion at *m/z* 399 [M+H$^+$]. LC-MS analysis of authentic DPA-714 gave a retention time, mass spectrum and fragmentation profile identical to those in microsomes extracts. The main MS-MS fragments come from the departure of the fluoroethoxy group (*m/z* 353), of the *N*-diethyl group (N($CH_2CH_3$)$_2$, *m/z* 326), of the diethylcarboxamide group ((CO)N($CH_2CH_3$)$_2$, *m/z* 299) and formally of an hydroxyl function (*m/z* 382, keto-enol equilibrium). The mass spectrum of M1, M2 and M4 exhibited a molecular ion at *m/z* 415, 16 Da higher than the molecular ion for DPA-714, consistent with the insertion of an oxygen atom and the formation of three different alcohol derivatives by hydroxylation. In comparison to DPA-714, fragmentation of the molecular

DMD Fast Forward. Published on October 12, 2012 as DOI: 10.1124/dmd.112.046342
This article has not been copyedited and formatted. The final version may differ from this version.



ion of M1, M2 or M4 generated the same product ions *m/z* 398, 369, 342 and 315 showing an increment of 16 Da consistent with the presence of a hydroxyl group in the parent molecule and retention of this group in the main fragment ions. These hydroxylations probably occurred at the "upper part of the molecule", the more likely position being the two methyl substituants of the phenyl ring (as evidenced by a fragment at *m/z* 397 corresponding to a loss of water (-18). M3 exhibited a molecular ion at *m/z* 371 (-28), in agreement with the loss of one ethyl group by *N*-deethylation and consistent with the preservation of the fragments *m/z* 299 and *m/z* 326. M5 exhibited a molecular ion at *m/z* 353 (- 46), in agreement with the loss of the fluoroethyl group by O-deethylation as attested by the loss of this group in the main fragment ions. M6a exhibited a molecular ion at *m/z* 431 (+32), consistent with the formation of a dihydroxylated derivative of DPA-714. M6b exhibited a molecular ion at *m/z* 387 consistent with *N*-deethylation (- 28) and hydroxylation (+ 16) of DPA-714.

The low mass of [$^{18}$F]DPA-714 administered to baboons prevented direct identification of metabolites in plasma by LC-MS. However incubating rat liver microsomes with DPA-714 and analysis by LC-MS identified two compounds having the same retention times as the radiometabolites detected in baboon plasma (Fig.6). These two *in vivo* radiometabolites corresponded to N-dealkyl derivatives of [$^{18}$F]DPA-714, [$^{18}$F]-M3 and [$^{18}$F]-M6b. The peaks detected between 2 and 3 min by UV-detection corresponded to the solvent front. The third *in vivo* radiometabolite was not detected in microsomes. However, based on the metabolism of zolpidem, a closely related analogue of DPA-714 (Pichard et al., 1995), this highly polar compound was likely issued from further oxidation in plasma of a hydroxylated metabolite to generate a carboxylic acid derivative ([$^{18}$F]-M7). From these findings, metabolic pathways for DPA-714 were proposed in Fig.7. The main oxidative metabolism of DPA-714 in liver microsomes likely occurred at the methyl of the pyrimidine moiety (hydroxylation), at the nitrogen (*N*-deethylation)

and oxygen atom (*O*-deethylation).

**Oxidation of DPA-714 by cDNA-expressed human P450s isoforms**

Microsomes expressing individual human P450s isoforms were used to test their ability to catalyze the oxidation of DPA-714. The fraction of each metabolite was determined using LC-MS (Fig.8). Human CYP3A4 exhibited the highest catalytic activity for the formation of M4 (9.3%, methyl-hydroxylation), M3 (7%, *N*-deethylation) and M5 (3.4%, *O*-deethylation) as in human liver microsomes (Table 2). CYP2D6 was able to convert significantly DPA-714 into M5 (2.32%, *O*-deethylation). Other human CYPs catalyzed the formation of one to four minor metabolites (less than 1%).

DMD Fast Forward. Published on October 12, 2012 as DOI: 10.1124/dmd.112.046342
This article has not been copyedited and formatted. The final version may differ from this version.



**Discussion**

The major findings of the present study are as follows. First, the main ways of elimination of [$^{18}$F]DPA-714 in baboons were the hepatobiliary (at least for the parent compound) and urinary (for radiometabolites) systems. Second, [$^{18}$F]DPA-714 was rapidly metabolized *in vivo* in rats and baboons into at least three radiometabolites. All of these were more polar than the native radioligand. Third, LC-MS-MS analysis of metabolites produced *in vitro* identified [M+H$^{+}$] ions consistent with hydroxyl, N- and O-deethyl derivatives of DPA-714. Two of them, deethyl and deethyl-hydroxyl derivatives of DPA-714, have the same retention times than those detected in baboon plasma. Fourth, evidence indicates that a small amount of an acidic [$^{18}$F]metabolite enters the rat brain at late times but does not appear to display specific binding. Fifth, we have developed a rapid and easy method of quantification of the radioligand and its radiometabolites in plasma by SPE that may be useful in human quantitative PET studies.

The peripheral *in vivo* biodistribution of [$^{18}$F]DPA-714 by whole body PET studies in baboon showed a high uptake of [$^{18}$F]DPA-714 in TSPO-rich peripheral regions such as the heart, spleen and kidneys in accordance with the data observed in rodents (Fookes et al., 2008, James, 2008) and recently in humans (Arlicot et al., 2012). The other peripheral organs identified with moderate or high levels of radioactivity were involved in the metabolism or excretion of the tracer such as liver and gallbladder. This radioactivity uptake has previously been shown to be specific by displacement experiments with non-labeled DPA-714 (James et al., 2008). Time-activity curves in the gallbaldder (data not shown) showed that the liver was a major route of elimination of [$^{18}$F]DPA-714 in baboons, with a finding also described in humans (Arlicot et al., 2012). Urine was a route of excretion for radiometabolites. Indeed, a very small amount of residual [$^{18}$F]DPA-714 was found in the urinary samples at 120 min p.i. A vertebral uptake of radioactivity was also observed in baboons as well as in humans (Arlicot et al., 2008).

DMD Fast Forward. Published on October 12, 2012 as DOI: 10.1124/dmd.112.046342
This article has not been copyedited and formatted. The final version may differ from this version.



The understanding of the metabolism of a candidate PET radioligand is important in establishing its value for quantitative imaging. Ideally, the candidate radioligand should not give rise to radiometabolite that can enter the brain and significantly impair the identity of the PET signal. After administration of [$^{18}$F]DPA-714 in baboons, the radioactivity represented by the non-metabolized radioligand decreased rapidly in plasma. This radioactivity was also composed of a highly polar radiometabolite and of two radiometabolites with intermediate retention times and lipophilicity. Similar rapid plasma decreases for radiotracers have been observed in baboons with other TSPO ligands, [$^{18}$F]FEDAA1106 (Zhang et al., 2004), [$^{18}$F]FEPPA (Wilson et al., 2008) and with the structurally similar analogues [$^{18}$F]PBR102 and [$^{18}$F]PBR111 (Fookes et al., 2008). In humans, [$^{18}$F]PBR06 and [$^{11}$C]PBR28 were shown to be rapidly metabolized in plasma (Dickstein et al., 2011) while [$^{18}$F]DPA-714 decreased slower (Arlicot et al., 2011).

The low mass of radioligand administered to baboons (a few nanomoles) prevented direct identification of metabolites in plasma using LC-MS. However, incubating liver microsomes with DPA-714 and analyses by LC-MS identified at least seven metabolites (M1 to M6b) in rat and human, four metabolites in baboon, two of them having the same retention times as the radiometabolites in baboon plasma. All were more polar than the native radioligand and in all except one, M5, the fluorine atom was preserved. At least four were the same in all three species but the relative amount of individual metabolites differed between species. LC-MS data also demonstrated the formation by cytochromes P450 in rat, baboon and human liver microsomes of seven main metabolites issued from *N*-deethylation ([$^{18}$F]-M3, *m/z* 371*)*, hydroxylations giving three alcohol derivatives ([$^{18}$F]-M1, [$^{18}$F]-M2, [$^{18}$F]-M4, *m/z* 415), di-hydroxlation ([$^{18}$F]-M6a *m/z* 431), *N*-deethylation and hydroxylations ([$^{18}$F]-M6b *m/z* 415) and *O*-deethylation ([$^{18}$F]-M5, *m/z* 353*)*.

Baboon microsomal studies suggested that the radiometabolites detected in plasma arose both from *N*-deethylation ([$^{18}$F]-M3) and N-deethylation plus hydroxylation ([$^{18}$F]-M6b). The third plasma radiometabolite ([18F]-M7) was not found in microsomal incubations and thus could not be identified by this technique. Based on the metabolism of zolpidem (Pichard et al., 1995), a closely structural analogue of DPA-714, this radiometabolite was proposed to be generated by further oxidation of a hydroxylated radiometabolite(s) in plasma leading to the formation of a carboxylic acid derivative ([$^{18}$F]-M7).

Human recombinant cytochromes P450 were used as a predictive model of human metabolism. CYP3A4 was found to be the major enzyme responsible for one hydroxylation reaction, *N*- and *O*-deethylation of DPA-714 as shown in cDNA-expressed human CYPs assays. CYP3A4 being the most abundant form in human liver, similar biotransformation of DPA-714 may occur *in vivo*. CYP2D6 was also clearly involved in the formation of *O*-deethylated DPA-714. The genetic polymorphism of human CYP2D6 may lead to large inter-individual variability.

*In vivo*, *O*-deethylation led to the formation of two metabolites: a non-labeled metabolite (M5) undetectable by radio-HPLC or LC-MS due to the low mass administered and [$^{18}$F]fluoroacetaldehyde which is further converted to [$^{18}$F]fluoroacetate (or fluoroacetic acid) and defluorinated into free [$^{18}$F]fluoride. This transformation should not be quantitatively important as shown by the low uptake of radioactivity in the bones (skull and vertebra). It should be noticed that red marrow is present in these bones and red marrow also contains TSPO (Kam WW Et al., 2012). Indeed PET cannot distinguish between free [$^{18}$F] trapped in the hydroxyapatite of bones and [$^{18}$F]DPA-714 binding to red marrow cells. The radioactivity found in the acetonitrile pellet increased with time, consistent with the formation of a radiometabolite likely [$^{18}$F]fluoroacetic acid during the biotransformation process of O-deethylation.

[$^{18}$F]fluoroacetate has been proposed as a radiotracer for prostate tumours and for imaging of glial

DMD Fast Forward. Published on October 12, 2012 as DOI: 10.1124/dmd.112.046342
This article has not been copyedited and formatted. The final version may differ from this version.



metabolism. This compound is known to be further converted to [$^{18}$F]fluoride (Tecle et al., 1989, Marik et al., 2009; Ponde et al., 2007; Nishii et al., 2012). In previous imaging studies in rodents the free [$^{18}$F]fluoride contributed to significant level of bone uptake in rodents after [$^{18}$F]DPA-714 administration (Fookes et al., 2008). The in vitro findings described in this paper demonstrating the formation by rat, baboon and human cytochromes P450 of O-dealkylated DPA-714 and thus [$^{18}$F]fluoroacetate. Our present results confirmed this hypothesis proposed. In our study, the measurement of the radioactivity in the rat tighbone and in the bone marrow showed a higher level of radioactivity (almost two-fold) in the bone marrow than in the cortical zone of the tighbone. This result, in accordance with previously published data (Fookes et al., 2008) may reflect TSPO expression in the bone marrow. The radioactivity in the cortical zone of the tighbone may result from the fixation of [$^{18}$F]fluoride, provided from [$^{18}$F]fluoroacetate generated by O-deethylation of the radioligand. In baboons, radioactivity uptake was observed in vertebra probably due to both specific uptake of radioactivity in the bone marrow and to the uptake of [$^{18}$F]fluoride in the bones. Different metabolic pathways and species differences have been described for [$^{18}$F]fluoroacetate (Nishii et al., 2011). The differences in the extent of defluorination of [$^{18}$F]-DPA-714 between species (Fookes et al., 2008, James et al., 2008, Arlicot et al., 2011) may be explained by a difference in the metabolism of the radioligand by O-deethylation and a difference in the metabolic pathways of fluoroacetate (Tecle et al., 1989).

Experiments were performed in rats to gain greater insight into the metabolism of [$^{18}$F]DPA-714 and the potential contribution of radiometabolites to the brain radioactivity. Radiometabolites appeared quite rapidly in rat plasma. No radiometabolite had been detected at early times, 10 min and 30 min post injection. [$^{18}$F]-M7 was detected in the brain at 120 min post injection. Ratios of *ex vivo* measurements of brain to plasma of [$^{18}$F]DPA-714 and [$^{18}$F]-M7 suggested the lack of specific accumulation of this radiometabolite.

DMD Fast Forward. Published on October 12, 2012 as DOI: 10.1124/dmd.112.046342
This article has not been copyedited and formatted. The final version may differ from this version.



Finally, a simplified method of quantification of [$^{18}$F]DPA-714 in plasma was developed using direct solid phase extraction in order to improve the estimation of a metabolite-corrected input function for future quantitative human PET studies. Similar exponential decrease of [$^{18}$F]DPA-714 in plasma was obtained with SPE and radio-HPLC, considered as the reference method. Compared to radio-HPLC, the main advantages of the SPE method were the higher sensitivity (increased by a factor 80), the fast processing (less than 30 min for more than 20 samples for SPE against 30 min for one time point by HPLC), the possibility to process simultaneously multiple low radioactivity samples even at late times of the PET scan and the low volume of plasma required. These advantages are particularly important in light of the decay of [$^{18}$F]-fluorine and the low activity injected to humans. Furthermore, this highly sensitive and specific procedure can be easily automated and used on a routine clinical basis. Another study by Katsifis et al. (2011) has also described a SPE method for measurement of intact TSPO ligands belonging to a closely related chemical family (PBR102 and PBR111). They also found a good agreement between the SPE and HPLC methods.

In conclusion, [$^{18}$F]DPA-714 is rapidly and extensively converted *in vivo* into several radiometabolites in rats and baboons. *In vitro* rat, baboon and human microsomal studies demonstrates the formation by cytochromes P450s of hydroxylated and deethylated metabolites, some of which are detected in rat and baboon plasma. Secondary oxidation in plasma of a [$^{18}$F] hydroxylated metabolite is likely to produce the main radiometabolite, which cross the rat blood brain barrier. *In vivo O*-deethylation generates an unlabelled compound concomitantly with [$^{18}$F]fluoroacetaldehyde, leading to formation of a small uptake of [$^{18}$F]fluoride in the bones. The SPE developed for the quantification of the non-metabolized fraction of [$^{18}$F]DPA-714 in plasma is the method of choice for the quantification in humans with low activity samples.

**Authorship contribution:**

*Participated in research design:* Peyronneau, Valette
*Conducted experiments:* Peyronneau, Valette, Saba, Goutal, Dollé, Damont, Bottlaender
*Contributed new reagents or analytic tools:* Peyronneau, Damont, Kassiou
*Performed data analysis:* Peyronneau, Saba, Goutal, Valette
*Wrote or contributed to the writing of the manuscript:* Peyronneau, Valette, Bottlaender

**References**

Arlicot N, Vercouillie J, Ribeiro MJ, Tauber C, Venel Y, Baulieu JL, Maia S, Corcia P, Stabin MG, Reynolds A, Kassiou M, Guilloteau D.(2012) Initial evaluation in healthy humans of [(18)F]DPA-714, a potential PET biomarker for neuroinflammation. *Nucl Med Biol* **39**:570-8.

Batarseh A and Papadopoulos V (2010) Regulation of translocator protein 18 kDa (TSPO) expression in health and disease states. *Mol Cell Endocrinol* **327**:1-12.

Boellaard R, Oikonen V, Hoffmann A, Van Berckel BNM, Windhorst AD (2011) Initial studies of [18F]DPA714 binding in patients with Alzheimer's disease and healthy controls. *Eur J Nucl Med Mol Imaging* **38** (Suppl 2):S107.

Chauveau F, Boutin H, Van Camp N, Dollé F, Tavitian B.(2008) Nuclear imaging of neuroinflammation: a comprehensive review of [$^{11}$C]PK11195 challengers. *Eur J Nucl Mol Imaging* **35**:2304-2319.

Chauveau F, Van Camp N, Dollé F, Kuhnast B, Hinnen F, Damont A, Boutin H, James M, Kassiou M, Tavitian B. (2009) Comparative evaluation of the translocator protein radioligands 11C-DPA-713, 18F-DPA-714 and 11C-PK11195 in a rat model of acute neuroinflammation. *J Nucl Med* **50**:468-476.

Chelli B, Lena A, Vanacore R, Da Pozzo E, Costa B, Rossi L, Salvetti A, Scatena F, Ceruti S, Abbracchio MP, Gremigni V, Martini C.(2004) Peripheral benzodiazepine receptor ligands:

mitochondrial transmembrane potential depolarization and apoptosis induction in rat C6 glioma cells. *Biochem Pharmacol* **68**:125-134.

Damont A-L, Hinnen F, Kuhnast B, Schöllorm-Peyronneau M-A, James M Luus C, Tavitian B, Kassiou M, Dollé F (2008) Radiosynthesis of [$^{18}$F]DPA-714, a selective radioligand for imaging the translocator protein (18 kDa) with PET. *J Labelled Comp Radiopharm* **51**:286-292.

Dickstein LP, Zoghbi SS, Fujimura Y, Imaizumi M, Zhang Y, Pike VW, Innis RB, **Fujita M** (2011) Comparison of 18F-and 11C-labeled aryloxyanilide analogs to measure translocator protein in human brain using positron emission tomography. *Eur J Nucl Med Mol Imaging* **38**:352-357.

Dollé F, Luus C, Reynolds A, Kassiou M. (2009) Radiolabelled molecules for imaging the translocator protein (18 kDa) using positron emission tomography. *Curr Med Chem* **16**:2899-2923.

Fookes CJ, Pham TQ, Mattner F, Greguric I, Loc'h C, Liu X, Berghofer P, Shepherd R, Gregoire MC, Katsifis A (2008) Synthesis and biological evaluation of substituted [$^{18}$F]imidazo[1,2-a]pyridines and [$^{18}$F]pyrazolo[1,5-a]pyrimidines for the study of the peripheral benzodiazepine receptor using positron emission tomography. *J Med Chem* **51**:3700-3712.

Hirvonen J, Roivainen A, Virta J, Helin S, Någren K, Rinne JO. (2010) Human biodistribution and radiation dosimetry of 11C-(R)-PK11195, the prototypic PET ligand to image inflammation. *Eur J Nucl Med Mol Imaging* 37:606-12.

James ML, Fulton RR, Vercoullie J, Henderson DJ, Garreau L, Chalon S, Dolle F, Costa B,

Guilloteau D, Kassiou M. (2008) DPA-714, a new translocator protein-specific ligand: synthesis, radiofluorination, and pharmacologic characterization. *J Nucl Med* **49**:814-822.

Kam WW, Meikle SR, Dunstan CR, Banati RB (2012) The 18 kDa Translocator Protein (Peripheral Benzodiazepine Receptor) Expression in the Bone of Normal, Osteoprotegerin or Low Calcium Diet Treated Mice. *PLoS One* **7**:e30623.

Katsifis A, Loc'h C, Henderson D, Bourdier T, Pham T, Greguric I, Lam P, Callaghan P, Mattner F, Eberl S, Fulham M.(2011) A rapid solid-phase extraction method for measurement of non-metabolised peripheral benzodiazepine receptor ligands, [$^{18}$F]PBR102 and [$^{18}$F]PBR111, in rat and primate plasma. *Nucl Med Biol* **38**:137-148.

Kremers P, Beaune P, Cresteil T, de Graeve J, Columelli S, Leroux JP, Gielen JE. (1981) Cytochrome P-450 monooxygenase activities in human and rat liver microsomes. *Eur J Biochem* **1**:118:599-606.

Lacapère JJ, Papadopoulos V (2003) Peripheral-type benzodiazepine receptor: structure and function of a cholesterol-binding protein in steroid and bile acid synthesis. *Steroids* **68**:569-585.

Lang S (2002) The role of peripheral benzodiazepine receptors (PBRs) in CNS pathophysiology. *Curr Med Chem* **9**: 1411-1415.

Marik J, Ogasawara A, Martin-McNulty B, Ross J, Flores JE, Gill HS, Tinianow JN, Vanderbilt AN, Nishimura M, Peale F, Pastuskovas C, Greve JM, van Bruggen N, Williams SP. (2009) PET of glial metabolism using 2-$^{18}$F-fluoroacetate. *J Nucl Med* **50**:982-990.

Myers R, Manjil LG, Cullen BM, Price GW, Frackowiak RS, Cremer JE (1991) Macrophage and astrocyte populations in relation to [$^{3}$H]PK 11195 binding in rat cerebral cortex following a local ischemic lesion. *J Cereb Blood Flow Metab* **11**:314-322.

Nishii R, Tong W, Wendt R 3rd, Soghomonyan S, Mukhopadhyay U, Balatoni J, Mawlawi O, Bidaut L, Tinkey P, Borne A, Alauddin M, Gonzalez-Lepera C, Yang B, Gelovani JG. (2012) Pharmacokinetics, Metabolism, Biodistribution, Radiation Dosimetry, and Toxicology of 18F-Fluoroacetate ((18)F-FACE) in Non-human Primates. *Mol Imaging Biol* **14**:231-224.

Omura T, Sato R (1964) The carbon monoxide binding pigment of liver microsomes. I. Evidence for its hemoprotein nature. *J Biol Chem* **239**:2370-2378.

Papadopoulos V, Baraldi M, Guilarte TR, Knudsen TB, Lacapère JJ, Lindemann P, Norenberg MD, Nutt D, Weizman A, Zhang MR, Gavish M.(2006) Translocator protein (18 kDa): new nomenclature for the peripheral-type benzodiazepine receptor based on its structure and molecular function. *Trends Pharmacol Sci* **27**:402-409.

Papadopoulos V, Lecanu L, Brown RC, Han Z, Yao ZX (2006) Peripheral-type benzodiazepine receptor in neurosteroid biosynthesis, neuropathology and neurological disorders. *Neurosciences* **138**:749-756.

Pichard L, Gillet G, Bonfils C, Domergue J, Thénot JP, Maurel P (1995) Oxidative metabolism of

zolpidem by human liver cytochrome P450s. *Drug Metab. Dispos*. **23**:1253-1262.

Ponde DA, Dence CS, Oyama N, Kim J, Tai YC, Laforest R, Siegel BA and Welch MJ (2007) 18F-fluoroacetate: a potential acetate analog for prostate tumor imaging--in vivo evaluation of $^{18}$F-fluoroacetate versus $^{11}$C-acetate. *J Nucl Med* **48**:420-428.

Rupprecht R, Papadopoulos V, Rammes G, Baghai TC, Fan J, Akula N, Groyer G, Adams D, Schumacher M (2010) Translocator protein (18 kDa) (TSPO) as a therapeutic target for neurological and psychiatric disorders. *Nat Rev Drug Discov* **9**:971-988.

Tecle B and Casida JE (1989) Enzymatic defluorination and metabolism of fluoroacetate, fluoroacetamide, fluoroethanol and (-)-erythro-fluorocitrate in rats and mice examined by 19F and 13C NMR. *Chem Res Toxicol* **2**:429-435.

Wilson AA, Garcia A, Parkes J, McCormick P, Stephenson KA, Houle S, Vasdev N.(2008) Radiosynthesis and initial evaluation of [18F]-FEPPA for PET imaging of peripheral benzodiazepine receptors. *Nucl Med Biol* **35**:305-314.

Zhang MR, Maeda J, Ogawa M, Noguchi J, Ito T, Yoshida Y, Okauchi T, Obayashi S, Suhara T, Suzuki K. (2004) Development of a new radioligand, N-(5-fluoro-2-phenoxyphenyl)-N-(2-[18F]fluoroethyl-5methoxybenzyl)acetamide, for pet imaging of peripheral benzodiazepine receptor in primate brain. *J Med Chem* **47**:2228-2235.

**Footnotes:**

The authors declare that they have no conflict of interest.

**Legends for Figures:**

**Fig 1**: Representative radiochromatogram of baboon plasma following injection of [$^{18}$F]DPA-714 (the numbers are retention times) and suggested radiometabolites.

**Fig 2**: **(A)** Time course of the fraction of unchanged [$^{18}$F]DPA-714 and radiometabolite [$^{18}$F]-M7 in baboon plasma (mean ± sd, n=6 independent PET experiments) determined by radio-HPLC. The results are expressed as a percent of total radioactivity (%). Experimental data were fitted as the sum of two exponentials (Origin V8.5). **(B)** [$^{18}$F] radioactivity in acetonitrile pellet. The results are expressed as a percent of total radioactivity (%). Experimental data were fitted as the sum of two exponentials (Origin V8.5). **(C)** Representative plasma time-activity curve after injection of [$^{18}$F]DPA-714 in one baboon.

**Fig 3**: **(A)** Time-course of the radioactivity in each SPE fractions (F1, F2, F3, F4) in baboon plasma. **(B)** Time course of the fraction of unchanged [$^{18}$F]DPA-714 in baboon plasma determined by radio-HPLC and SPE (mean ± sd, n=3 independent experiments). Comparison of radio-HPLC and solid-phase extraction to determine the time-dependant decrease of the fraction of non-metabolized [$^{18}$F]DPA-714. Data points were fitted as a mono-exponential decrease (Origin V8.5).

**Fig 4**: Plasma and brain biodistribution of total [$^{18}$F] radioactivity, unchanged [$^{18}$F]DPA-714 and [$^{18}$F]-M7 in rats at 120 min post injection of [$^{18}$F]DPA-714. The concentrations of unchanged [$^{18}$F]DPA-714 and [$^{18}$F]-M7 were measured by radio-HPLC and expressed as a percent of the injected dose per gramme of tissue (% ID/g). Values are the mean ± sd of 2 independent

experiments (with 2 rats by experiment).

**Fig. 5**: **(A)** Analysis of metabolites of DPA-714 in rat and human liver microsomal incubations by HPLC, **(B)** *In vitro* metabolism of DPA-714 in different species: comparison of the rates of formation of DPA-714 metabolites in rat, baboon and human liver microsomes (30 min incubation) and expressed as nmol metabolite per mg of microsomal proteins per min. Values are the mean ± sd of n=5 independent duplicate experiments.

**Fig. 6**: Comparison of the metabolic profile of baboon plasma (radio-HPLC) and rat liver microsomal incubations (UV-HPLC).

**Fig 7**: Proposed metabolic pathways for DPA-714 and its main metabolites in liver microsomes based on LC-MS and MS-MS experiments.

**Fig 8:** Human CYPs responsible of the biotransformation of DPA-714: comparison with human liver microsomes. The percentage of each metabolite is expressed as a percent of total area as detected by HPLC LC-UV/MS. Values are the mean of n=3 independent duplicate experiments. Errors on each measure were lower than 10% for metabolites representing more than 1% of total peak area and around 20% or less for metabolites representing more than 1% of total peak area.

DMD Fast Forward. Published on October 12, 2012 as DOI: 10.1124/dmd.112.046342
This article has not been copyedited and formatted. The final version may differ from this version.



**Tables**

**Table 1:** Biodistribution of [$^{18}$F]DPA-714 in one baboon. SUV(s)max values were obtained from dynamic wholebody PET acquisition,

| Target organ | SUV(s)max |
|---|---|
| Lung | **5.67** |
| Heart | **7.42** |
| Liver | **6.28** |
| Gallbladder | **7.31** |
| Spleen | **7.57** |
| Kidney | **12.7** |
| Urinary bladder | **6.50** |
| Parotid | **1.93** |
| Vertebra | **1.99** |

DMD Fast Forward. Published on October 12, 2012 as DOI: 10.1124/dmd.112.046342
This article has not been copyedited and formatted. The final version may differ from this version.



**Table 2**: Microsomal metabolites of DPA-714 (r, rat; b, baboon; h, human).

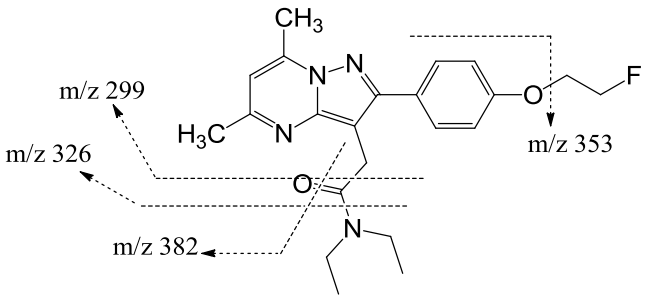


| Metabolites | Rt | [M+H+] | Main fragments | Species |
|---|---|---|---|---|
| M1 | 16.87 | 415 (+16) | 398, 369, 342, 315 | r, (h) |
| M2 | 16.43 | 415 (+16) | 398, 369, 342, 315 | r, b, h |
| M3 | 16.10 | 371 (-28) | 354, 325, 326, 299 | r, b, h |
| M4 | 15.85 | 415 (+16) | 398, 369, 342, 315 | r, b, h |
| M5 | 15.05 | 353 (-46) | 336, 307, 280, 253 | (r), b, h |
| M6a | 14.28 | 431 (+32) | 414, 385, 358, 331 | r |
| M6b | 13.88 | 387 (-12) | 370, 235, 342, 315 | r, (h) |

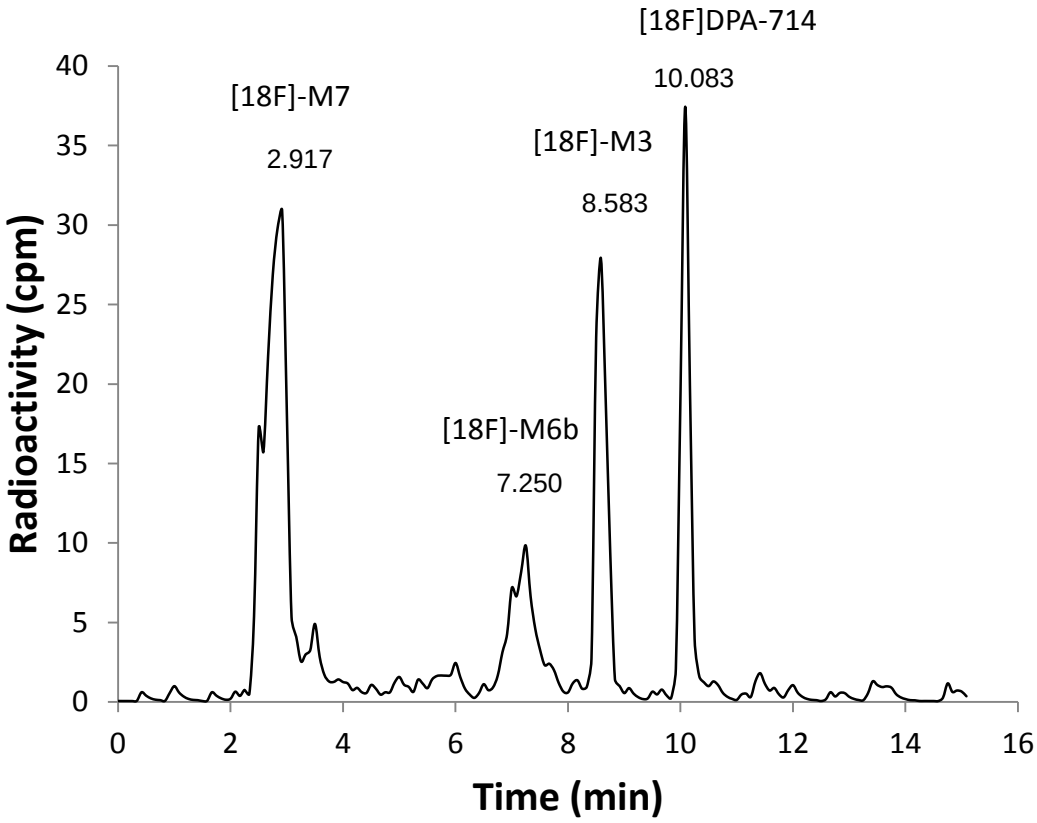


Figure 1

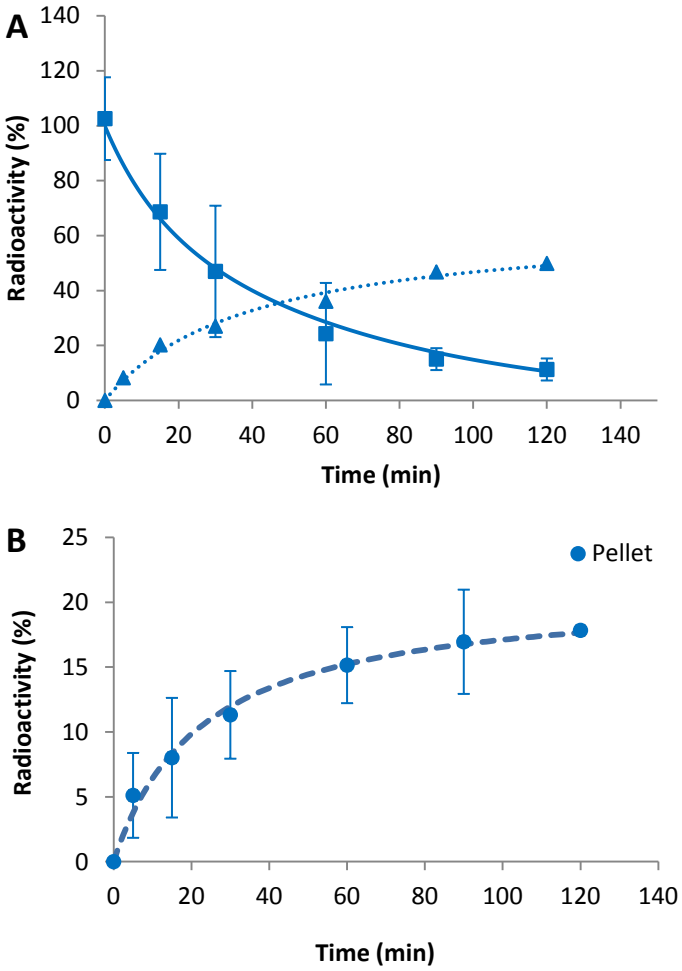




Figure 2

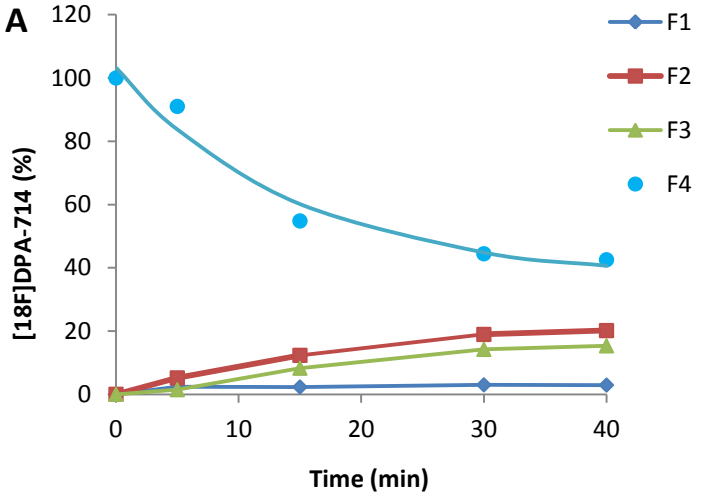


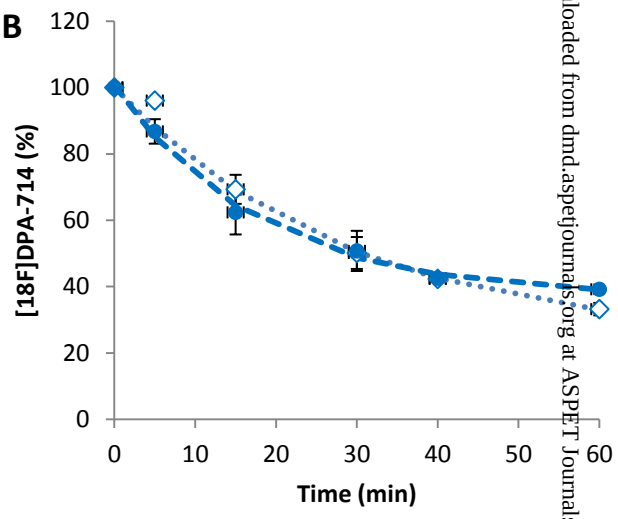


| Analytical Method | Model | ExpDec1 | | T1/2 (min) |
|---|---|---|---|---|
| | Equation | y = A1*exp(-x/t1) + y0 | | |
| **SPE** | y0 | 36.8840737 | 2.49049613 | 12 |
| | A1 | 63.7827442 | 2.66512361 | |
| | t1 | 17.8404643 | 2.18365963 | |
| **HPLC** | y0 | 23.6104663 | 0.99496187 | 19 |
| | A1 | 76.5011336 | 0.97622818 | |
| | t1 | 28.6334419 | 0.84871661 | |



Figure 3

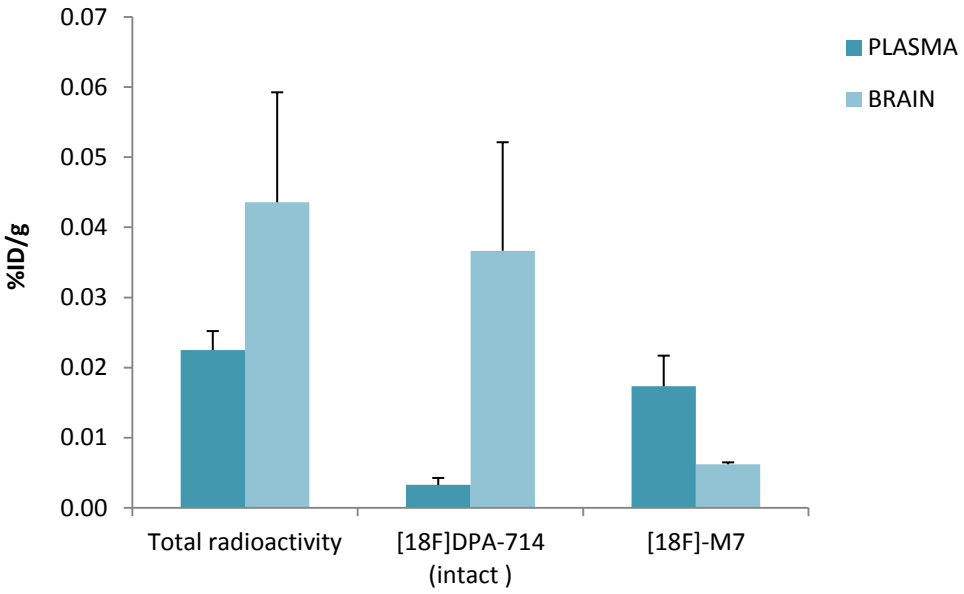


Figure 4

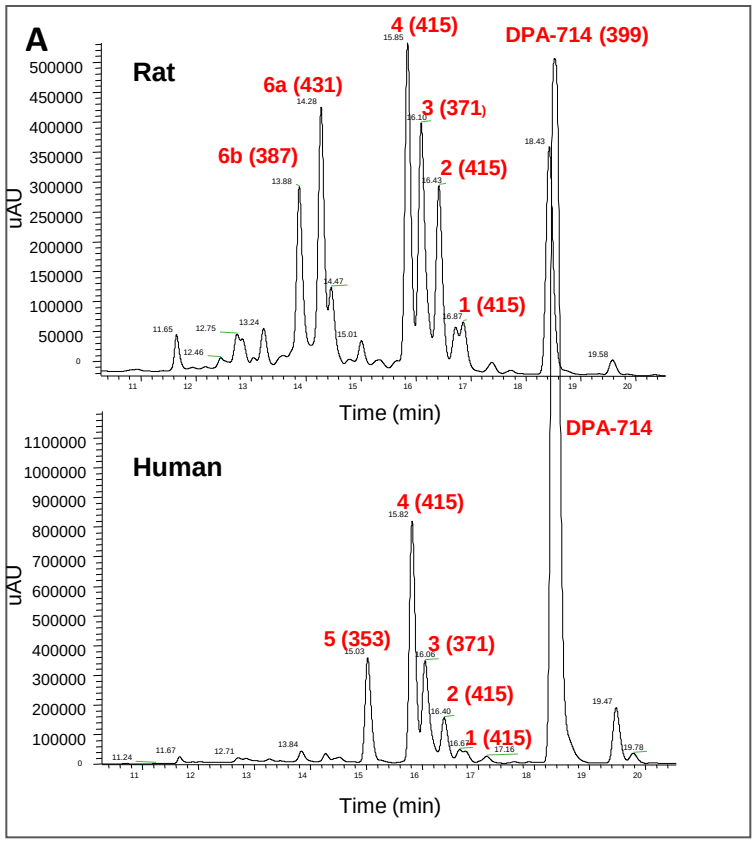


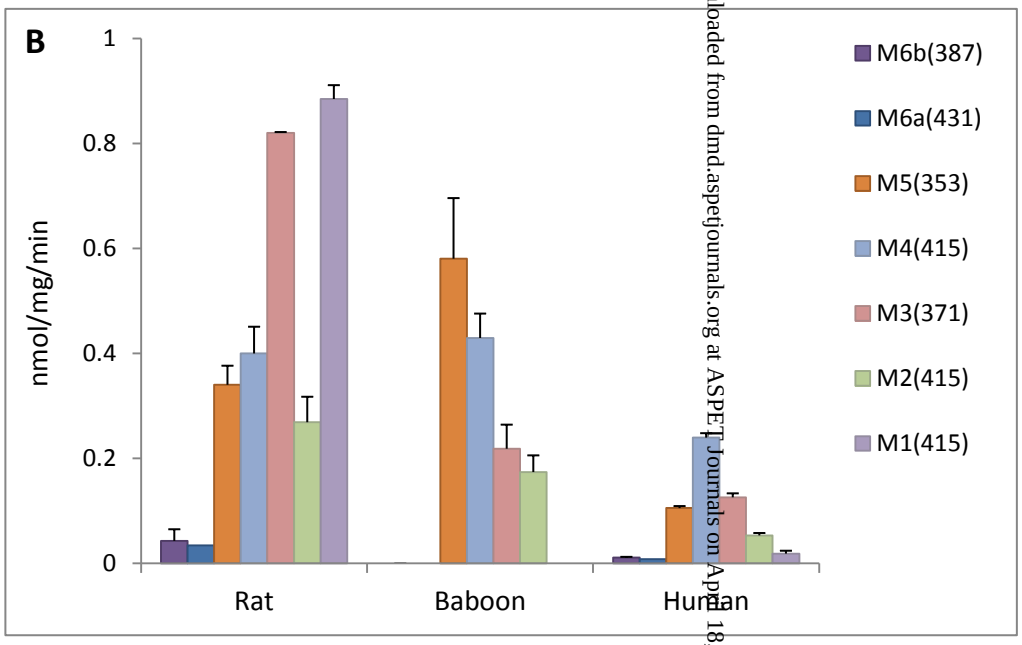




Figure 5

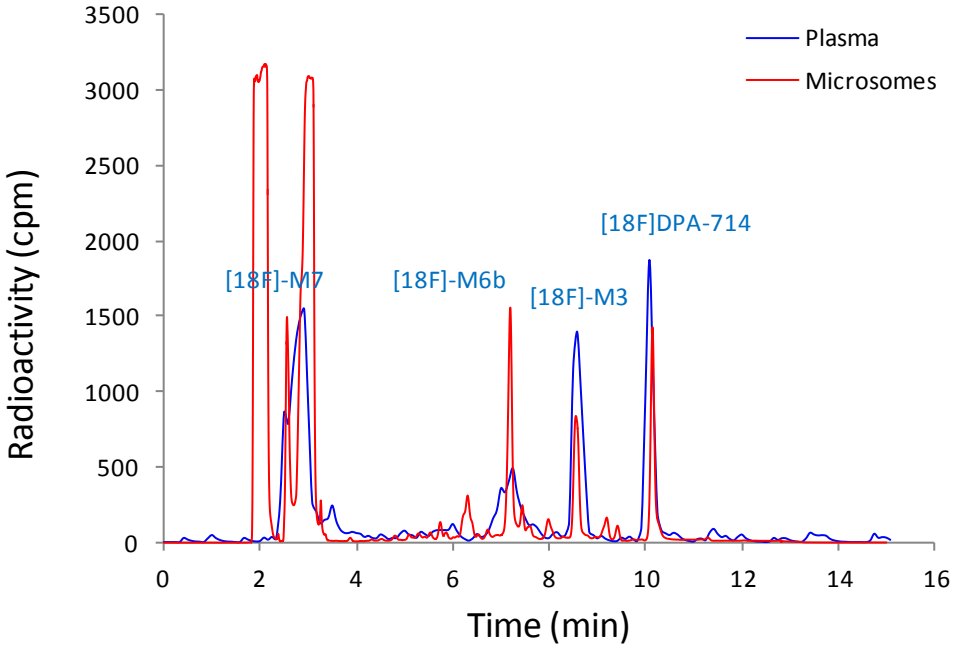


Figure 6

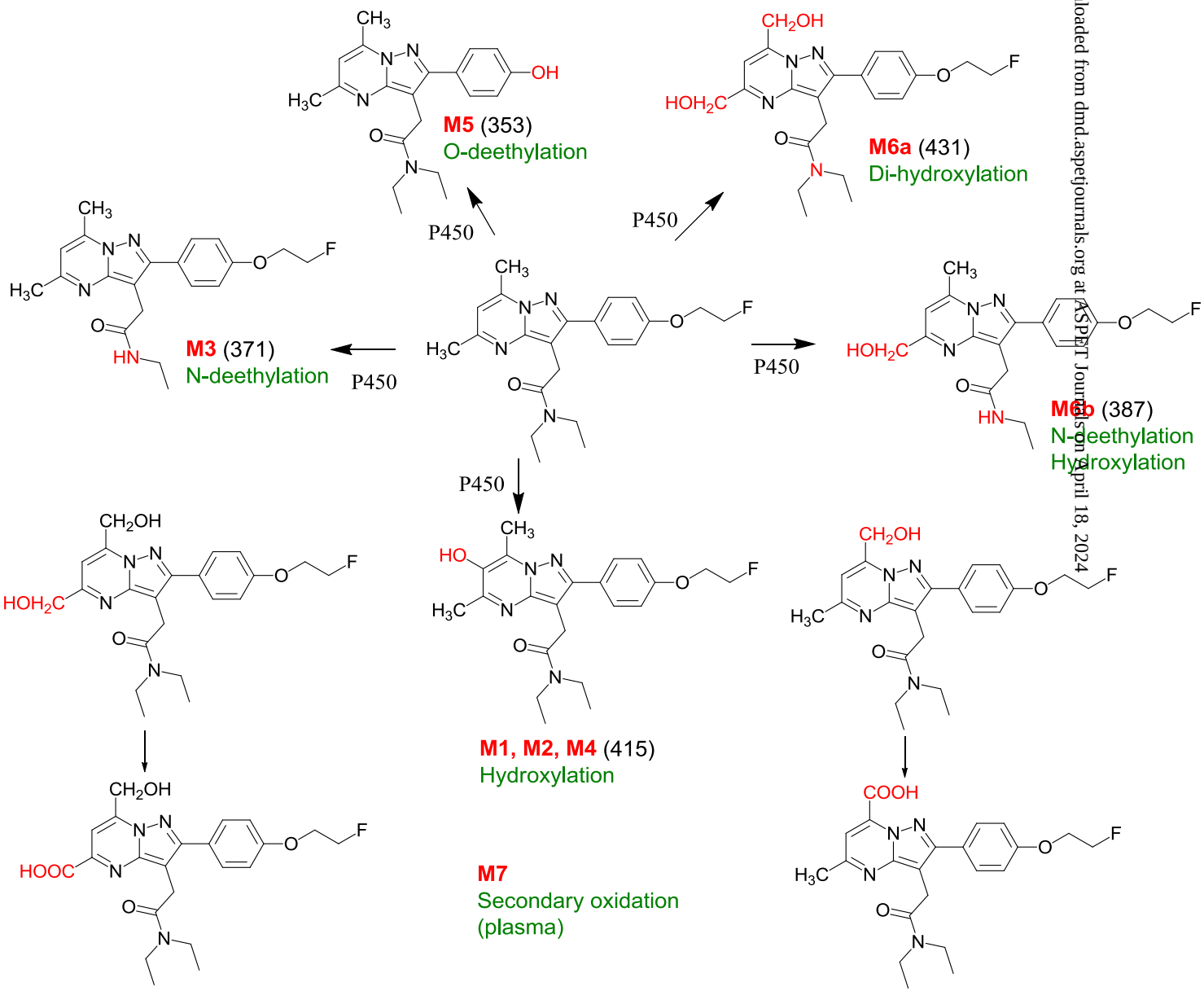


Figure 7

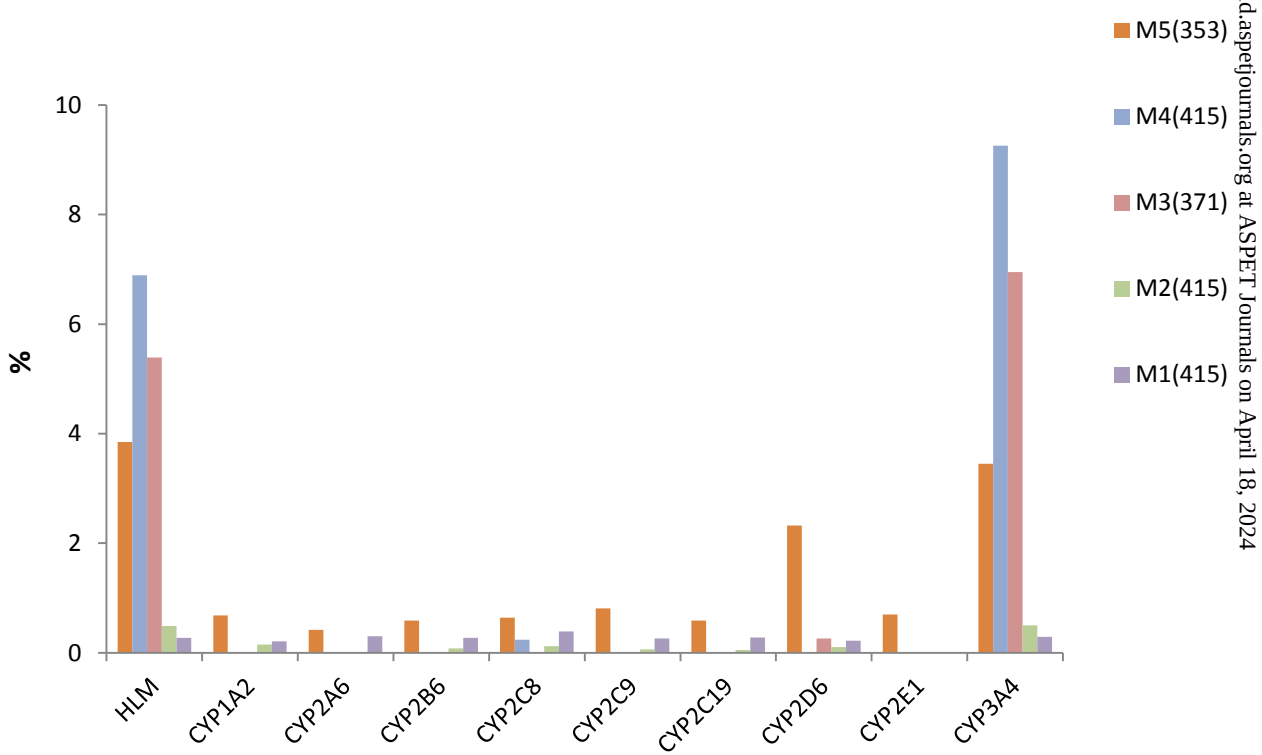


Figure 8